Department of Energy

Washington, DC 20585

QA: N/A
DOCKET NUMBER: 63-001

January 28, 2010

ATTN: Document Control Desk
John H. (Jack) Sulima, Project Manager
Project Management Branch B
Division of High-Level Waste Repository Safety
Office of Nuclear Material Safety and Safeguards
U.S. Nuclear Regulatory Commission
EBB-2B2
11545 Rockville Pike
Rockville, MD 20852-2738

YUCCA MOUNTAIN - REQUEST FOR ADDITIONAL INFORMATION - SAFETY
EVALUATION REPORT, VOLUME 3 - POSTCLOSURE CHAPTER 2.2.1.3.2,
MECHANICAL DISRUPTION OF ENGINEERED BARRIERS, 3RD SET - (DEPARTMENT
OF ENERGY'S SAFETY ANALYSIS REPORT SECTION 2.3.4)

Reference: Ltr, Sulima to Williams, dtd 12/14/2009, "Yucca Mountain – Request for
               Additional Information – Safety Evaluation Report, Volume 3 – Postclosure
               Chapter 2.2.1.3.2, Mechanical Disruption of Engineered Barriers, 3rd Set –
               (Department of Energy's Safety Analysis Report Section 2.3.4)"

The purpose of this letter is to transmit the U.S. Department of Energy's (DOE) response to the
remaining one (1) of the nine (9) Requests for Additional Information (RAI) identified in the
above-referenced letter. The response to RAI Number 1 is provided as an enclosure to this letter.
DOE submitted the responses to RAI Numbers 5, 6, 8, and 9 on January 7, 2010; the response to
RAI Number 7 on January 12, 2010; and the responses to RAI Numbers 2, 3, and 4 on
January 19, 2010.

The DOE references cited in the RAI response have previously been provided with the License
Application.

There is one commitment in the enclosed RAI response. If you have any questions regarding this
letter, please contact me at (202) 586-9620, or by email to jeff.williams@rw.doe.gov.

Jeffrey R. Williams, Supervisor
Licensing Interactions Branch
Regulatory Affairs Division
Office of Technical Management

OTM:CJM-0254

Enclosure:

    Response to RAI Volume 3, Chapter 2.2.1.3.2, Set 3, Number 1

cc w/encls:
J. C. Chen, NRC, Rockville, MD
J. R. Cuadrado, NRC, Rockville, MD
J. R. Davis, NRC, Rockville, MD
R. K. Johnson, NRC, Rockville, MD
A. S. Mohseni, NRC, Rockville, MD
N. K. Stablein, NRC, Rockville, MD
D. B. Spitzberg, NRC, Arlington, TX
J. D. Parrott, NRC, Las Vegas, NV
L. M. Willoughby, NRC, Las Vegas, NV
Jack Sulima, NRC, Rockville, MD
Christian Jacobs, NRC, Rockville, MD
Lola Gomez, NRC, Rockville, MD
W. C. Patrick, CNWRA, San Antonio, TX
Budhi Sagar, CNWRA, San Antonio, TX
Beverly Street, CNWRA, San Antonio, TX
Rod McCullum, NEI, Washington, DC
B. J. Garrick, NWTRB, Arlington, VA
Bruce Breslow, State of Nevada, Carson City, NV
Alan Kalt, Churchill County, Fallon, NV
Irene Navis, Clark County, Las Vegas, NV
Ed Mueller, Esmeralda County, Goldfield, NV
Ron Damele, Eureka County, Eureka, NV
Alisa Lembke, Inyo County, Independence, CA
Chuck Chapin, Lander County, Battle Mountain, NV
Connie Simkins, Lincoln County, Pioche, NV
Linda Mathias, Mineral County, Hawthorne, NV
Darrell Lacy, Nye County, Pahrump, NV
Jeff VanNeil, Nye County, Pahrump, NV
Joe Kennedy, Timbisha Shoshone Tribe, Death Valley, CA
Mike Simon, White Pine County, Ely, NV
K. W. Bell, California Energy Commission, Sacramento, CA
Barbara Byron, California Energy Commission, Sacramento, CA
Susan Durbin, California Attorney General's Office, Sacramento, CA
Charles Fitzpatrick, Egan, Fitzpatrick, Malsch, PLLC

EIE Document Components:

001_Trans_Ltr_3.2.2.1.3.2_Set_3_RAI_1.pdf
002_Encl_3.2.2.1.3.2_Set_3_RAI_1.pdf   3,804 KB

RAI Volume 3, Chapter 2.2.1.3.2, Third Set, Number 1:

Demonstrate that the drip shield retains adequate seepage barrier functionality after deformation (SAR 2.3.4.5.3).

Basis: DOE concludes that the drip shield continues to function as a barrier to seepage after the drip shield framework collapses (SNL 2007ay; Section 6.12.2). SAR Section 2.3.4.5.3.3.2 concludes that the drip shield plates in the crown will remain intact after the framework legs buckle because they are structurally more robust than the framework. The SAR, however, does not discuss how an appropriate level of uncertainty for framework collapse (including spatial variability) has been considered. Neither does the SAR demonstrate that failures due to high stress concentrations in the collapsed Titanium Grade 7 plates are unlikely to occur or that seepage water inflow through deformed drip shields (e.g., discontinuities) will not affect performance significantly.

Analyses also show that for an intact drip shield framework (i.e., no uniform corrosion), the bulkhead snaps through in the middle of the crown span during failure (SAR, 2.3.4.5.3.3.2). The SAR does not explain the apparent inconsistency between the analyses used to generate the drip shield abstractions for the first tens of thousands of years, and the conclusion that the crown plates are structurally more robust than the framework legs (SAR Sections 2.3.4.5, 2.3.4.5.3.3.2, and 2.3.4.4.4.1), particularly in the context of barrier functionality.

1. RESPONSE

After collapse of its sidewalls, the drip shield still maintains the capability to function as a seepage barrier. Two cases illustrate this point: completely collapsed sidewalls and partly collapsed sidewalls. Because the crown remains intact even after complete collapse of the sidewalls, the drip shield maintains its seepage barrier function. In addition, dynamic analysis of the structural response to the ground motion confirms that snap-through of the crown is not an appropriate failure mode for the performance assessment.

The potential impact from partly collapsed sidewalls has been evaluated. The specific case of a drip shield whose sidewalls collapse at one end but remain intact (standing) at the other end has been chosen to represent the uncertainty in framework collapse from spatial variability. The results of numerical calculations estimate the strain concentrations in the crown plates if one end of the drip shield collapses onto the waste package beneath it but the other end remains standing. A total system performance assessment (TSPA) sensitivity calculation provides additional insight into the effect on mean annual dose if early plate failures were to occur from partial collapse of the sidewalls.

Section 1.1 of this response describes the features of the drip shield design that structurally reinforce the crown relative to the sidewalls and the different material properties for the Titanium Grade 24[1] framework versus the Grade 7 plates. Section 1.2 explains why the drip shield with collapsed sidewalls retains its ability to deflect seepage, and explains the apparent inconsistency in failure mode for the as-installed drip shield. Section 1.3 documents the numerical calculations that evaluate the potential for plate rupture after partial collapse of the drip shield. Section 1.4 discusses the uncertainty in plastic load capacity for the crown plates and a sensitivity calculation demonstrating that seepage water inflow through earlier failures of the crown plates has negligible impact on mean annual dose.

1.1   KEY FEATURES OF THE DRIP SHIELD DESIGN

1.1.1   Drip Shield Design Reinforces the Crown

As shown in Figure 1, the drip shield consists of a framework of bulkheads and beams that support the plates, which are welded to the framework. Five bulkheads and one peripheral bulkhead divide the crown of the drip shield into five sections (or segments). The sidewalls of the drip shield are also divided into five sections by the four large support beams, a support beam connector, and the drip shield connector plate. As used in this response, the term "sidewalls" or "legs" refers to Plate-2 (see Figure 1), the large support beams on Plate-2, and the external support plates welded to Plate-2. Each of the five sections has similar components and similar mechanical stiffness, a fact that has been used to simplify the three-dimensional structural response calculations for the drip shield.

The crown of the drip shield is highly reinforced by the design shown in Figure 1. For example, the five bulkheads supporting the crown plate (Plate-1 in Figure 1) are 902.8 mm high and 38.1 mm thick. Each bulkhead also has a bottom flange that is 20 mm thick. These bulkheads and flanges provide a stiff framework under vertical and lateral (i.e., perpendicular to the drift axis) loading.
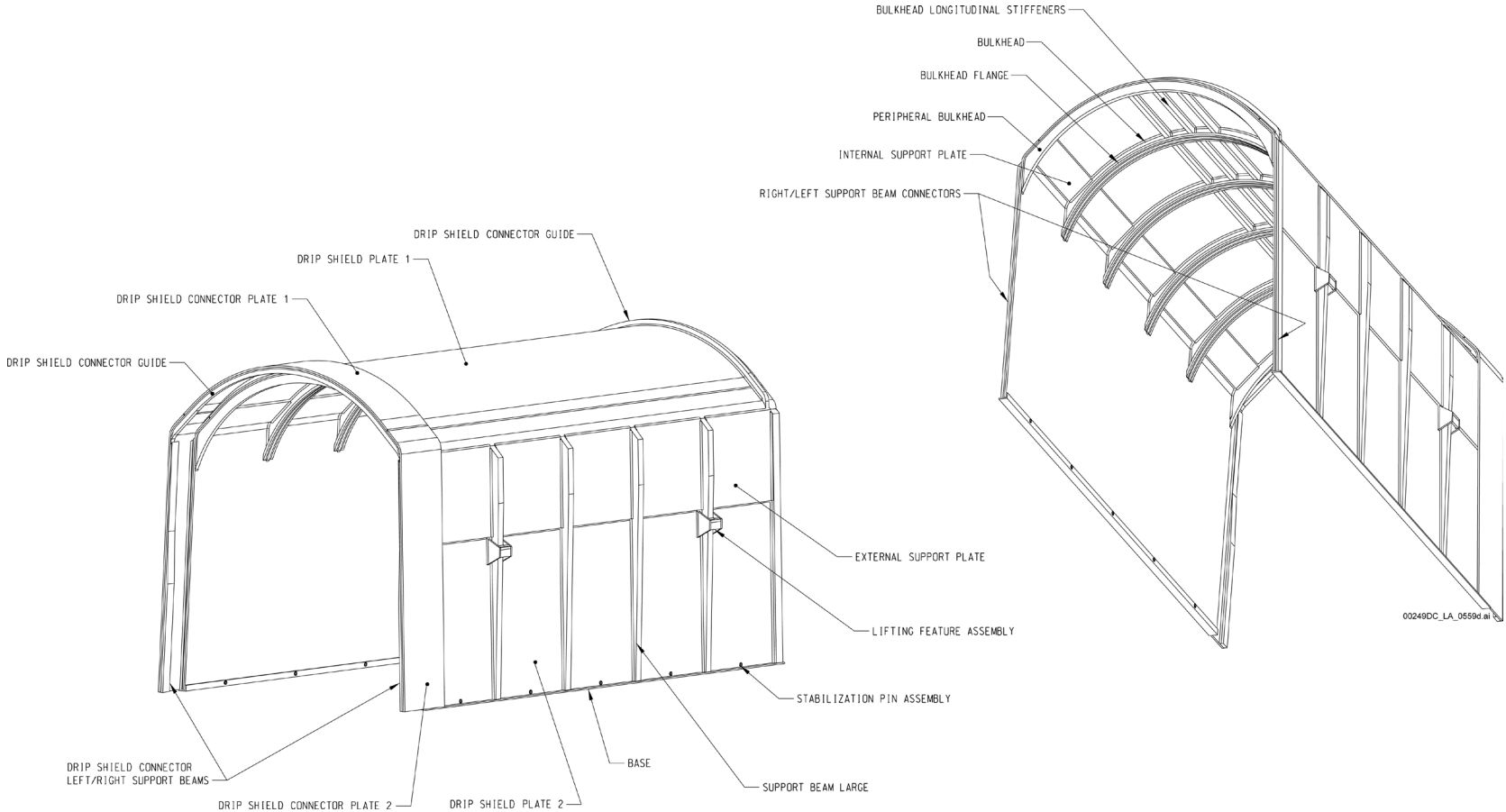
The crown is also reinforced in the longitudinal direction (i.e., axially along the length of the drip shield). Figure 2 provides an expanded view of the individual components of the drip shield, and identifies the components that provide extra reinforcement. First, the crown of the drip shield is reinforced axially by three bulkhead longitudinal stiffeners that are 70 mm by 38 mm in cross section. Second, the sides of the crown are reinforced axially by ten internal support plates, which are 12.7 mm thick and welded to Plate-1, the top plate of the drip shield that is 15 mm thick. This provides almost a double thickness of Titanium Grade 7 along the sides of the crown where it meets the shoulders. The presence of the interior support plates has been conservatively ignored in the calculations of plate fragility, but is relevant to this response. Third, the sidewalls of the drip shield are axially reinforced by ten external support plates, which are 12.7 mm thick

---

[1] Calculations in *Mechanical Assessment of Degraded Waste Packages and Drip Shields Subject to Vibratory Ground Motion* (SNL 2007a) use Titanium Grade 24 as a proxy for Titanium Grade 29, which is the current design material for the drip shield framework. Section 4.1.5 (SNL 2007a) has a comparison of material properties between Titanium Grade 24 and Titanium Grade 29.

and welded to the top of Plate-2, the sidewall of the drip shield that is 15 mm thick. This provides almost a double thickness of Titanium Grade 7 at the top of the sidewalls, where they meet the shoulder.

The five bulkheads, bulkhead longitudinal stiffeners, ten internal support plates, and ten external support plates stiffen the crown of the drip shield relative to its sidewalls. In effect, the crown and shoulders form a stiff box frame relative to the sidewalls, helping to explain why the crown and its plates remain intact even when the sidewalls buckle near the bottom of the drip shield (SAR Section 2.3.4.5.3.2.3, bottom of last paragraph).

BULKHEAD LONGITUDINAL STIFFENERS

BULKHEAD

BULKHEAD FLANGE

PERIPHERAL BULKHEAD

INTERNAL SUPPORT PLATE

RIGHT/LEFT SUPPORT BEAM CONNECTORS

DRIP SHIELD CONNECTOR GUIDE

DRIP SHIELD PLATE 1

DRIP SHIELD CONNECTOR PLATE 1

DRIP SHIELD CONNECTOR GUIDE

EXTERNAL SUPPORT PLATE

LIFTING FEATURE ASSEMBLY

STABILIZATION PIN ASSEMBLY

DRIP SHIELD CONNECTOR
LEFT/RIGHT SUPPORT BEAMS

DRIP SHIELD CONNECTOR PLATE 2

DRIP SHIELD PLATE 2

BASE

SUPPORT BEAM LARGE

00249DC_LA_0559d.ai

Source: SAR Figure 1.3.4-14.

Figure 1.   Components of the Interlocking Drip Shield
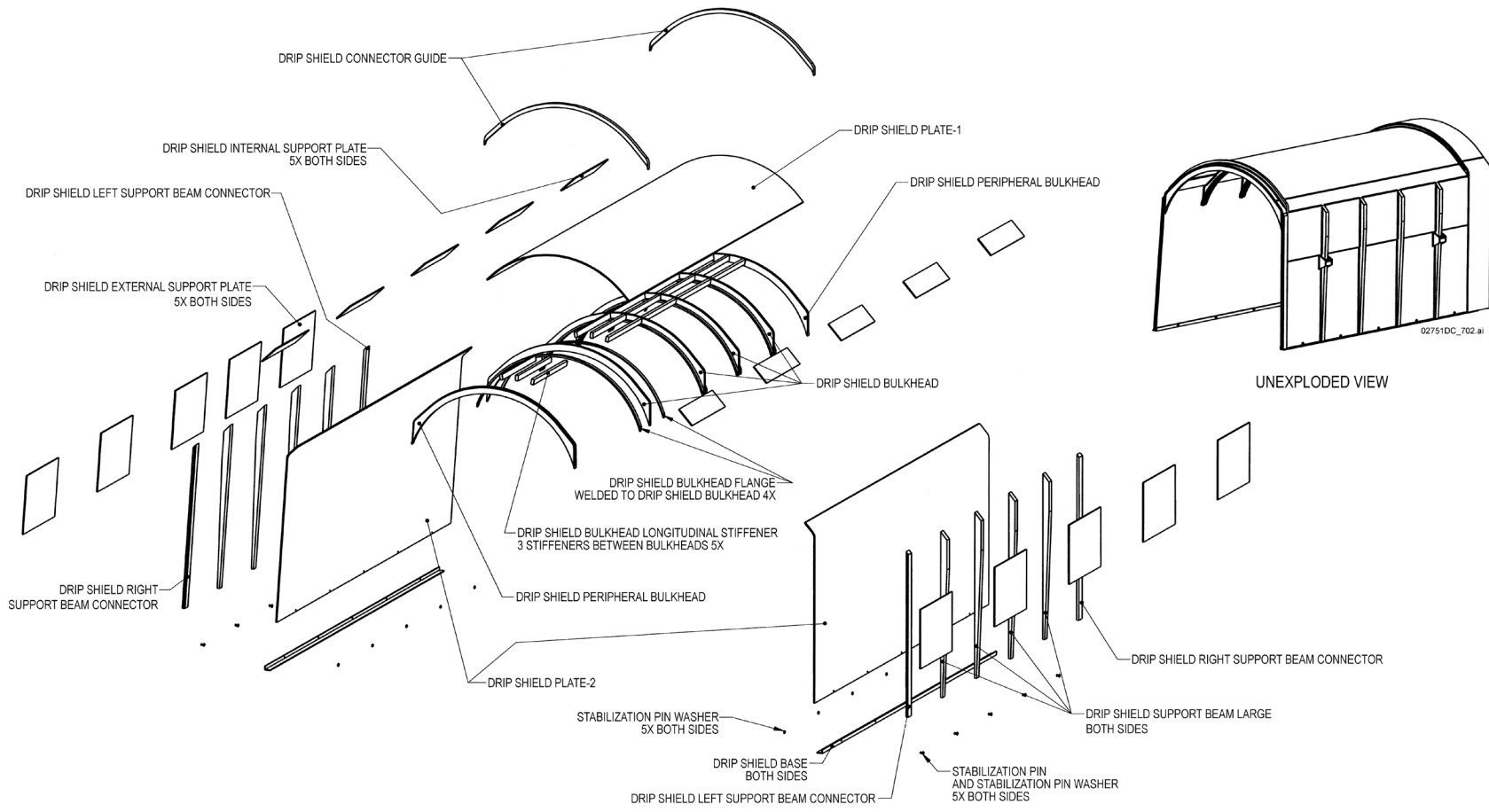
RAI: 3.2.2.1.3.2-3-00

Figure 2.   Sub-Assembly for the Individual Components of the Interlocking Drip Shield

1.1.2   Framework Bears the Load

The mechanical properties of the drip shield materials are important for the distribution of loads and strains within the structure. The plates are fabricated from Titanium Grade 7 and the framework components are fabricated from Titanium Grade 29. Grade 29 is used for the framework components because it is stronger and stiffer than Grade 7.

Figure 3 presents a comparison of the uniaxial stress-strain response at 60°C of Grade 7 and Grade 24, the proxy for Grade 29 in the structural response calculations. These curves demonstrate that, for a given strain, a uniaxial bar of Grade 24 will sustain more than twice the stress and bear more than twice the load than a bar of Grade 7, all other factors being equal. Alternately, at a stress of 400 MPa, Grade 24 still is elastic but the Grade 7 is essentially at ultimate failure. Figure 3 illustrates that Grade 24 is stronger and stiffer than Grade 7. This is not meant to imply that a component made from Grade 7 will always fail before a component made from Grade 24 because the component thicknesses have a major impact on structural response.
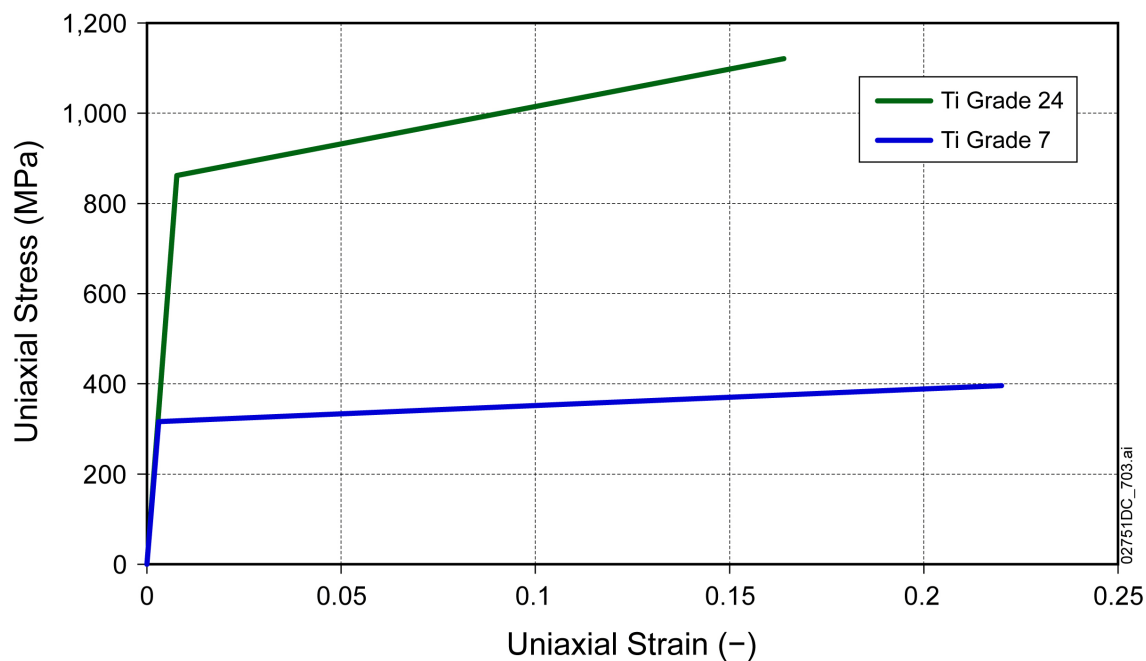

Figure 3.   Comparison of Uniaxial Stress-Strain Curves for Titanium Grades 7 and 24 at 60°C

These stress-strain curves also demonstrate that a bar of Grade 7 does not reach ultimate failure until a significantly greater ultimate strain than a bar of Grade 24. (The point of ultimate failure corresponds to the end point of each curve in Figure 3.) By design, the framework components in the crown of the drip shield will tend to bear more load than the plates. These statements are not precise because the bulkheads, axial stiffeners, and plates all have different thicknesses, cross sectional areas, curvature, etc., but it does provide insight into the dynamic response of the sidewalls versus the crown assembly and its plates, discussed in the next section.

1.2   RESPONSE WITH COMPLETELY COLLAPSED SIDEWALLS

1.2.1   Crown Assembly Remains Intact under Dynamic Loading

A series of two-dimensional dynamic simulations of a drip shield surrounded by the rubble were performed to evaluate the failure modes of the drip shield surrounded by seismically induced rockfall (SAR Section 2.3.4.5.3.3.3 and SNL 2007a, Section 6.4.4.5). The calculations were performed for four ground-motion sets at each of the 2.44 m/s and 4.07 m/s peak ground velocity (PGV) levels, using three drip shield configurations representing different levels of general corrosion: as-installed (no corrosion), 5-mm thickness reduction for all components, and 10-mm thickness reduction for all components. The four strongest sets of ground-motion time histories, numbers 3, 7, 9, and 13, were chosen from the 17 sets available at each PGV level for these calculations (SNL 2007a, Section 6.4.4.5). These choices maximize the rockfall load and structural response for the dynamic calculations.

These simulations provide a more accurate representation of interaction between the rubble and the drip shield and the dynamic rubble loads on the drip shield than the quasi-static analyses discussed in SAR Section 2.3.4.5.3.3.2. The dynamic simulations were two-dimensional and carried out by applying the vertical component and one horizontal component of each ground-motion set to a two-dimensional cross section of the drip shield in a fully collapsed drift. These calculations automatically generate the transient vertical and lateral rockfall loads on the drip shield, accounting for the complex interactions between the deforming structure and the moving mass of rubble.

The two-dimensional representations of the drip shield, which include the crown plates, bulkheads, and large support beams, are an approximation of the three-dimensional structure. The two-dimensional representations were designed to match or underestimate the flexural stiffness and bending moment versus curvature of the three-dimensional structure in the two-dimensional model (SNL 2007a, Section 6.4.4.3 and Appendix B). In other words, the two-dimensional representation is designed to underestimate the load bearing capacity of the three-dimensional structure (for the same static loading conditions).

The dynamic nature of the rubble loading, the selection of the two highest PGV levels and four strongest sets of ground motions, and the mechanical properties of the two-dimensional representation are designed to maximize the structural response of the drip shield in general and its crown in particular. If the crown and its plates are observed to remain intact under these dynamic analyses, then the crown is expected to remain intact and continue to fulfill its function as a barrier to seepage. In other words, the dynamic simulations bound the structural response of the drip shield for all relevant seismic events.

The results from the 24 dynamic calculations are summarized in SAR Section 2.3.4.5.3.3.3. Typically, the drip shield is observed to fail by buckling of a sidewall near the bottom, approximately 20 to 30 cm from the contact with the invert. This behavior is not surprising because the thickness of the large support beams is smallest at the bottom of the sidewalls and because the sidewall plates, Plate-2 in Figure 1, are not reinforced at their bottoms with external

support plates, only at their tops. This behavior is also reasonable because the crown and its plates form a stiff "box" relative to the sidewalls.

These fully dynamic simulations also demonstrate that the drip shield does not fail as a result of snap-through in the middle of the crown. Only for ground motion set number 11 at the 4.07 m/s PGV level are there indications of failure in the crown (for example, see SAR Figure 2.3.4-85). However, these potential crown failures occur at or near the shoulder, and not in a snap-through mode (SAR Figure 2.3.4-85 and SNL 2007a, Section 6.4.4.6, Figures 6-60 and 6-62). In this situation, any seepage through possible crown ruptures would result in flow down the side of the drip shield and not cause advective flow through the waste packages.

The dynamic two-dimensional simulations therefore confirm that the crown remains intact as a barrier to seepage with fully collapsed sidewalls, even for the maximum seismic ground motions.

1.2.2   Apparent Inconsistency in Failure Mode for As-Installed[2] Drip Shield

The three-dimensional quasi-static calculations for the ultimate plastic load capacities of the drip shield framework and of the crown plates demonstrate that the crown plates are structurally more robust than the framework legs, as stated in SAR Section 2.3.4.5.3.2.3. Figure 4 provides a side-by-side comparison of the plastic load capacities, also called limit loads in the SAR, from the information in SAR Figures 2.3.4-81 and 2.3.4-83. The comparison in Figure 4 demonstrates that the plastic load capacities of the crown plates are always greater than the plastic load capacities of the framework for the three levels of corrosion thinning, providing the basis for the statement that the crown plates are structurally more robust than the framework. In addition, the difference in load capacity is consistently represented in the fragility curves for the framework and crown plates because, for a given level of corrosion thinning, the probability of rupture of the crown plates is always lower than the probability of the sidewalls buckling at a given ground motion level (SAR Tables 2.3.4-43 and 2.3.4-44).

The three-dimensional quasi-static analyses also show that the failure mode for the as-installed drip shield is snap-through of the crown at the middle of its span (SAR Figure 2.3.4-82 and SAR Section 2.3.4.5.3.3.2). This failure mode is different than the failure mode for the two-dimensional dynamic calculations discussed in SAR Section 2.3.4.5.3.3.3. As explained in Section 1.2.1 of this response, the two-dimensional dynamic calculations typically fail by buckling of a sidewall near the bottom, approximately 20 to 30 cm from the contact with the invert, rather than by snap-through of the crown (SNL 2007a, Figure 6-60). Only one case in the dynamic two-dimensional calculations, ground-motion set number 11 at the 4.07 m/s PGV level, shows indications of failure in the crown. However, these potential crown failures occur at or near the shoulder, and do not exhibit a snap-through response (SAR Figure 2.3.4-85 and SNL 2007a, Section 6.4.4.6, Figures 6-60, 6-61, and 6-62). In this situation, any seepage through these crown failures would flow down the side of the drip shield and not cause advective releases from the waste packages.

---

[2] The term "As-Installed" means a drip shield whose thickness has not been reduced by corrosion. The term should not be construed to mean that some Engineered Barrier System (EBS) components have been installed.
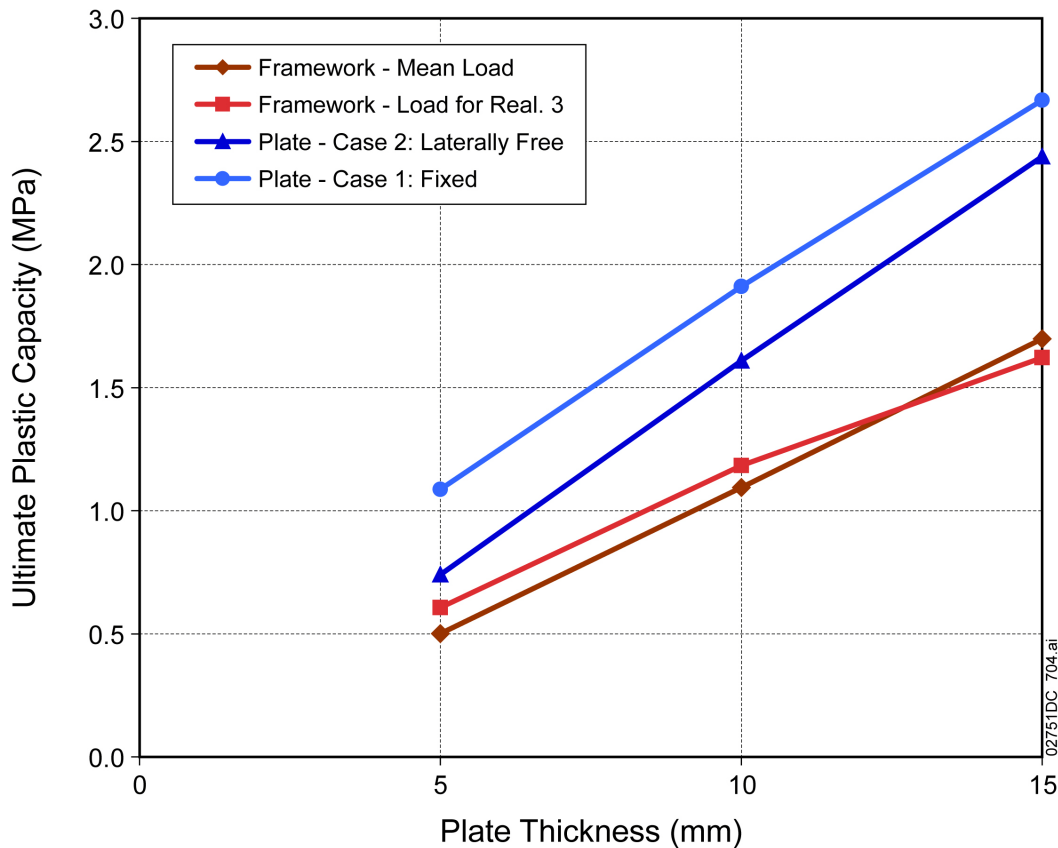
Figure 4.   Comparison of Ultimate Plastic Load Capacity (limit load) for the Drip Shield Framework and Drip Shield Crown Plates

The quasi-static analysis is designed to represent the main aspects of the drip shield–rubble interaction during strong seismic ground motions. The quasi-static analysis is expected to underestimate the load-bearing capacity of the drip shield during strong seismic ground motion because the peak value of the ground acceleration during a seismic ground motion occurs during a very brief time interval, while the equivalent quasi-static simulation applies a constant vertical load that is correlated with the peak (maximum) vertical ground acceleration, as discussed in the response to RAI 3.2.2.1.3.2-3-007. In effect, the quasi-static simulation is using the maximum vertical ground acceleration as a constant load on the drip shield and, therefore, underestimates load-bearing capacity. The quasi-static model also approximates the lateral loads on the drip shield, based on the displacement of the drip shield and the elastic properties of the surrounding rubble.

The two-dimensional dynamic calculations provide a more accurate representation of the transient rubble loads on the drip shield than the quasi-static model. The dynamic calculations determine the transient rockfall loads as a function of the ground motions in the lateral and vertical directions and as a function of structural displacements of the drip shield. The dynamic calculations therefore provide a more accurate and direct representation of the structural response

to ground motion during a seismic event, and provide a more accurate estimate of drip shield failure modes than the quasi-static model.

In this situation, the two-dimensional dynamic calculations have been used to verify that the quasi-static approach provides a reasonable and conservative representation of the ultimate plastic load capacity of the drip shield framework and to confirm that snap-through of the crown was not the appropriate failure mode for performance assessment. The results from the dynamic calculations described in Section 1.2.1 of this response and in SAR Section 2.3.4.5.3.3.3 are consistent with this description. However, the current text in SAR 2.3.4.5.3.3.3 contains a minor error in a description of the results of the quasi-static analysis results, and text has been proposed to correct the error (Section 3 of this response).

1.3 LOCALIZED FAILURE OF A SINGLE DRIP SHIELD

1.3.1   Drip Shield Separation and Its Impact on the Seepage Barrier

The potential for axial and vertical separation between adjacent drip shields is discussed in feature, event, or process (FEP) 1.2.03.02.0B, Seismic-Induced Rockfall Damages EBS Components. Drip shield separation is defined as an axial or vertical gap or space between two adjacent drip shields that allows in-drift seepage to flow directly onto waste packages. Separation is important because it negates the functionality of the drip shields as a barrier to seepage.

Axial separation of adjacent drip shields is excluded from the TSPA model because: (1) ground motion amplitudes that are sufficient to cause axial separation are also large enough to partially or completely collapse drifts in the repository, (2) rockfall begins within the first second or two of the arrival of these large amplitude ground motions, and (3) a kinematic study indicates that small static loads from rubble or frictional loads between EBS components are sufficient to eliminate axial separation of drip shields (SNL 2007b, Section 6.7.3.1). In this situation, rockfall provides restraints on the motion of the drip shields, preventing differential motion that could lead to separation. Axial separation is thus excluded from the TSPA model based on low probability.

Vertical separation of adjacent drip shields is also excluded from the TSPA model because: (1) rockfall provides restraints on the motion of the drip shields, preventing differential motion that could lead to separation, as discussed above, and (2) the drip shield connector subassemblies provide a 320-mm-long (12.6-inch-long) overlap at the joint between adjacent drip shields (SNL 2007b, Section 6.7.3.2). This overlap will protect the waste packages from direct seepage and direct rockfall that might result from a vertical displacement of a few inches between adjacent drip shields. In addition, the curved plates on the crown will continue to shed seepage laterally, and the connector guide and drip shield connector assembly provide an additional barrier to any seepage that is able to flow longitudinally toward the gap between shields. Vertical separation is not included in the TSPA model on the basis of low probability.

1.3.2   Numerical Analysis of a Partly Collapsed Drip Shield

The collapse of one end of the drip shield may impose significant loads that could potentially rupture the longitudinal stiffeners and plates in the crown, allowing seepage direct access to the waste package. Conceptually, this could occur if the welds that attach large support beams to the sidewalls fail, substantially weakening one end of the drip shield, and/or if the rockfall load is significantly greater on one end of the drip shield than the other end. A numerical analysis has been performed for the effective plastic strain in the crown plate for a partly collapsed drift shield. This analysis determines the potential for plate rupture as a function of the displacement of one section of the drip shield relative to adjacent sections of the drip shield.

The potential for differential displacements along the drip shield to cause rupturing or tearing of the drip shield crown plate has been investigated numerically. The numerical analysis is two-dimensional, along a vertical plane through the crown of the drip shield. The crown plate (i.e., Plate-1) is represented as a flat plate resting on the bulkheads. The curvature of Plate-1 in the out-of-plane direction is neglected, and the presence of the three longitudinal stiffeners is conservatively neglected.

During the numerical analysis, the bulkhead on one side of the plate is moved vertically downwards at relatively small velocity (to ensure quasi-static response in the analysis), simulating uneven deformation (i.e., collapse) of the drip shield framework; the other bulkhead is kept fixed. The boundary conditions on the bulkheads are fixed for rotation and horizontal translation during the simulation. This configuration overpredicts strain in the plate because plate stresses will cause rotation and horizontal translation of the bulkhead, thereby reducing stresses and strains in the plate. The bulkhead flange is not included in this modelling exercise.

The contours of the plastic shear strain in a 15-mm-thick plate after 19.8-cm differential displacement are shown in Figures 5 and 6 (detail). This differential displacement corresponds to the point of rupture, when the maximum effective strain equals the ultimate strain. The plastic strains are localized at the contact between the plate and the bulkhead.
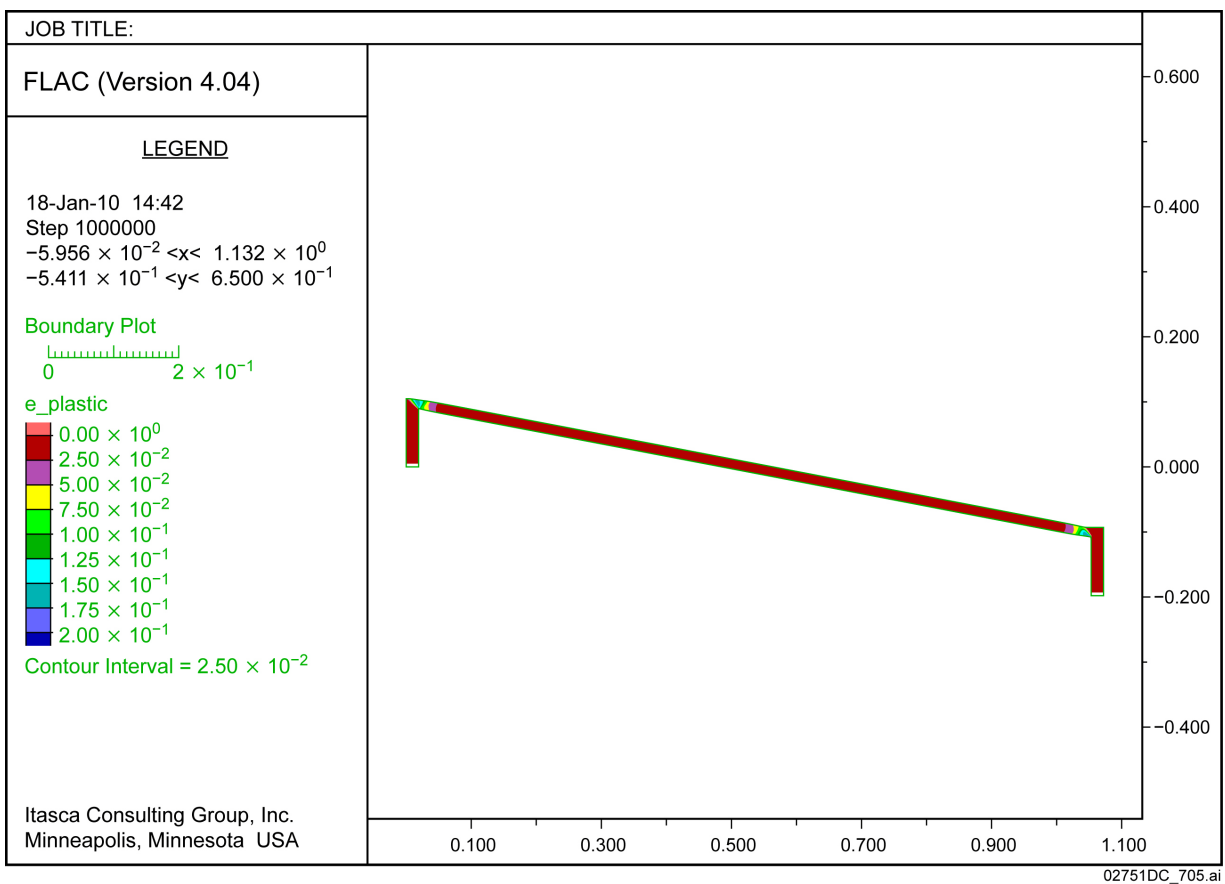
JOB TITLE:

FLAC (Version 4.04)

LEGEND

18-Jan-10 14:42
Step 1000000
-5.956×10^{-2} <x< 1.132×10^{0}
-5.411×10^{-1} <y< 6.500×10^{-1}

Boundary Plot

0   2×10^{-1}

e_plastic
0.00×10^{0}
2.50×10^{-2}
5.00×10^{-2}
7.50×10^{-2}
1.00×10^{-1}
1.25×10^{-1}
1.50×10^{-1}
1.75×10^{-1}
2.00×10^{-1}
Contour Interval = 2.50×10^{-2}

Itasca Consulting Group, Inc.
Minneapolis, Minnesota USA

0.100   0.300   0.500   0.700   0.900   1.100

0.600
0.400
0.200
0.000
−0.200
−0.400

02751DC_705.ai

Figure 5.   Plastic Shear Strains in 15-mm-Thick Plate after 19.8-cm Differential Displacement

JOB TITLE:

FLAC (Version 4.04)

LEGEND

18-Jan-10 14:42
Step 1000000
 9.602×10^{-1} <x< 1.117×10^{0}
 -2.189×10^{-1} <y< -6.229×10^{-2}

Boundary Plot

 0   2×10^{-1}

e_plastic
 0.00×10^{0}
 2.50×10^{-2}
 5.00×10^{-2}
 7.50×10^{-2}
 1.00×10^{-1}
 1.25×10^{-1}
 1.50×10^{-1}
 1.75×10^{-1}
 2.00×10^{-1}
Contour Interval = 2.50×10^{-2}

Itasca Consulting Group, Inc.
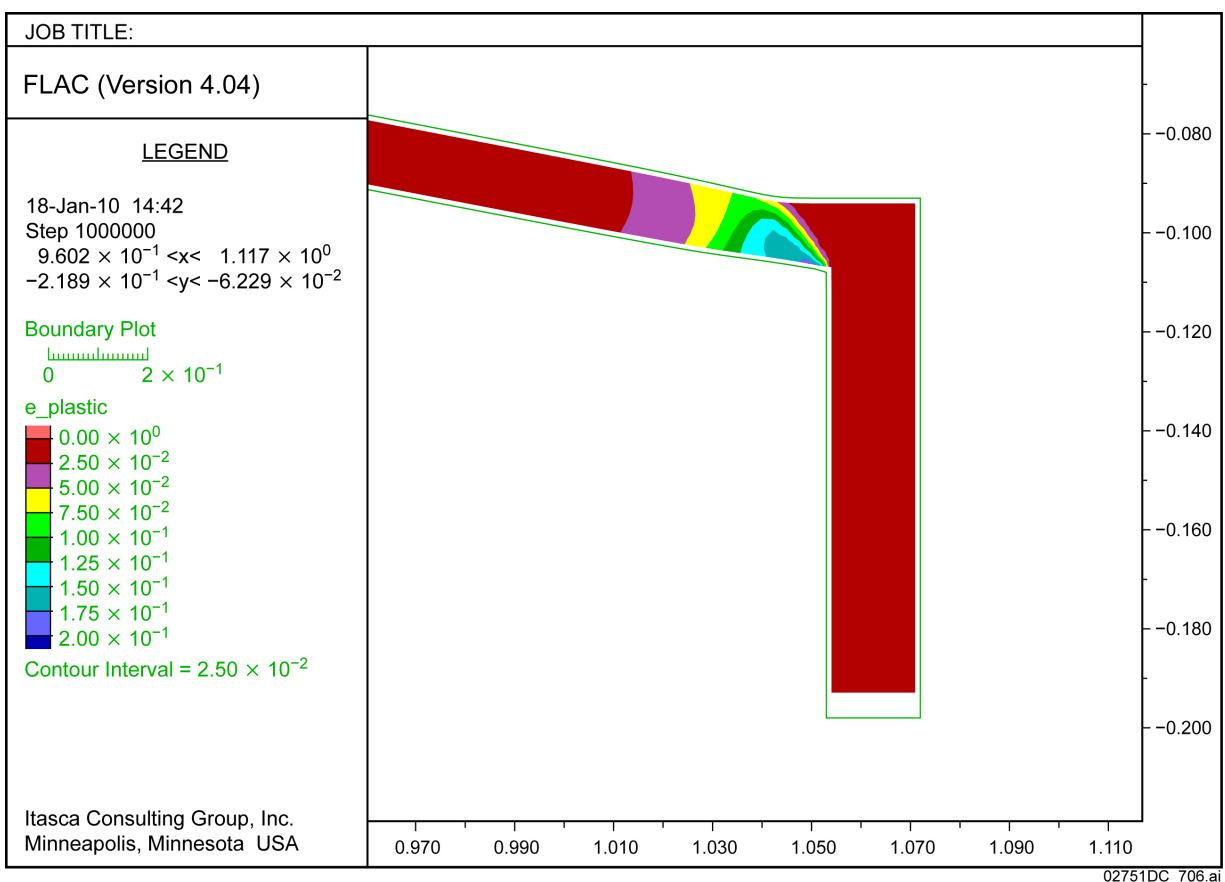Minneapolis, Minnesota USA

02751DC_706.ai

Figure 6.   Plastic Shear Strains in 15-mm-Thick Plate after 19.8-cm Differential Displacement

The evolution of the maximum effective plastic strain as a function of differential settlement is shown in Figure 7. The calculations were performed for three plate thicknesses (15 mm, 10 mm, and 5 mm), representing different stages of thickness reduction due to uniform corrosion. (In all calculations the dimensions of the bulkhead were the same as those in the initial configuration because the effect of thinning of the bulkhead on strains in the plate is negligible.)   The maximum plastic strain does not depend on the plate thickness, particularly for strain levels close to the rupture strain, because the calculation is driven by a displacement boundary condition. The analysis shows catastrophic failure at an effective plastic strain of about 60%. However, rupture of Titanium Grade 7 plate occurs at an ultimate true elongation of 21.7% (SNL 2007a, Table A-1). (The effective plastic strains in Figure 7 are compared with ultimate plastic strain of 21.7% (SNL 2007, Table 6-134), which corresponds to the ultimate true elongation of 22%.) The calculations therefore indicate that tearing of the plates will take place after about 18.9-cm differential displacements for a 15-mm-thick crown plate. The critical differential displacement for 10-mm- and 5-mm-thick plates is 18.8 cm and 18.2 cm, respectively.
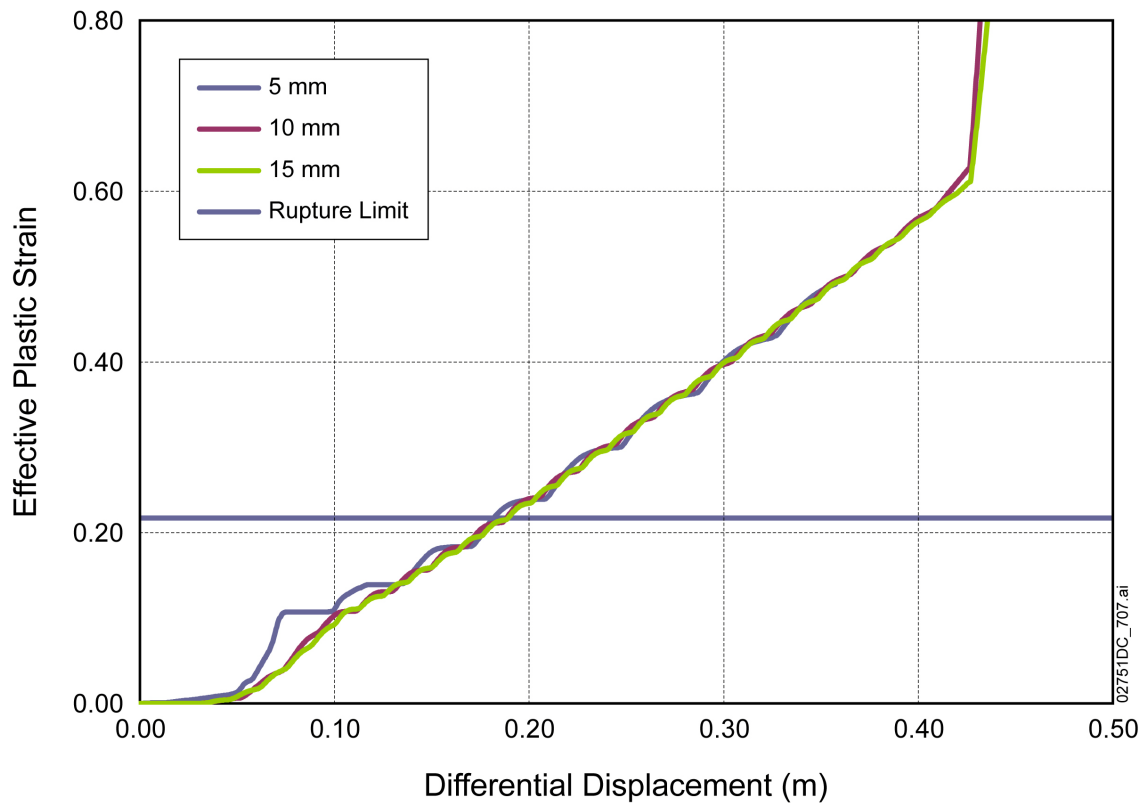
Figure 7. Effective Plastic Strain in Plates of Different Thicknesses as a Function of Differential Displacement

The numerical analysis imposes increasing differential displacement between bulkheads as the boundary condition for the analysis. The main mechanism that can cause differential displacement along the drip shield is partial collapse of the drip shield. Collapse of the drip shield framework typically occurs as a result of buckling of its legs (SNL 2007a, Sections 6.4.3.2.3 and 6.4.4.6 and Figures 6-55, 6-56, 6-60, 6-61, and 6-62). The vertical displacements of the drip shield before the legs buckle are relatively small. In addition, the static loads that cause drip shield collapse are relatively large (SNL 2007a, Figure 6-57) compared to the rubble loads in a completely collapsed drift (SNL 2007a, Table 6-136). Thus, there are two conditions necessary for drip shield collapse: (1) completely collapsed emplacement drift (to maximize the static rockfall load), and (2) strong seismic ground motions (to maximize the dynamic amplification of the static load).

Under conditions (1) and (2), the dynamic load on a single drip shield will be relatively uniform. First, the height of the rubble above a single drip shield will be relatively uniform when the drip shield collapses. If there is uneven rubble above a single drip shield at the start of a ground motion, the strong seismic ground motion that is required to collapse the drip shield will cause total collapse of any intact portions of the drift and even out the height of the rubble above the drip shield. Second, seismic amplification of the static rubble load will be almost uniform along the length of drip shield because the wave length of the ground motions is generally much

greater than the length of the drip shield. It follows that the dynamic load on a single drip shield will be relatively uniform.

Partial collapse of some segments of a drip shield while others fail is therefore unlikely because the dynamic loads in a collapsed drift will be relatively uniform and because the crown of the drip shield is a reinforced three-dimensional structure in the axial and lateral directions, as discussed in Section 1.1.1. If one or two segments collapse, additional load is transferred to the remaining, stable segments due to action of the longitudinal stiffeners and due to rubble load redistribution to stiffer and stronger sections of the drip shield. The transferred load is then likely to fail the remaining segments of the drip shield.

Even if partial collapse of a few drip shield segments occurs, the ductility of the drip shield crown plate is sufficient to allow substantial differential displacement before rupture occurs. Figure 8 illustrates a case with total collapse of the segment at one end of the drip shield, progressive collapse of the three intermediate segments, and no collapse for the segment on the other end of the drip shield. The numerical analyses show that the plates remain intact until 3×18.2 cm = 55 cm of total displacement over the three segments shown in Figure 8. (The critical displacement of 18.2 cm, obtained for a plate thickness of 5 mm, is used here as the smallest between 3 plate thicknesses analyzed.) For comparison, the clearance between the top of a waste package and the bottom of the drip shield varies between 14 inches (35.56 cm) to 27 inches (68.58 cm) (SNL 2007b, Table 4.1 and Section 6.11.1). While the displacement of 55 cm is less than the maximum clearance of 68.58 cm, it is likely that other processes, such as settlement of the drip shield into the invert backfill during a strong seismic ground motion, will accommodate this 13.5 cm difference.
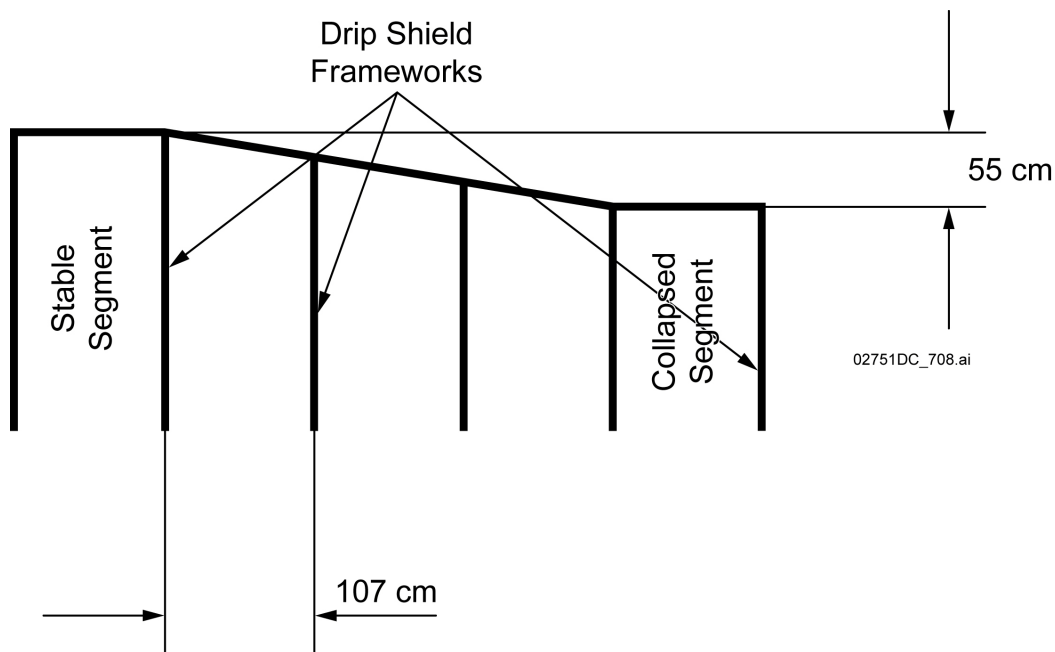

Figure 8.   Schematic Drawing of a Partially Collapsed Drip Shield

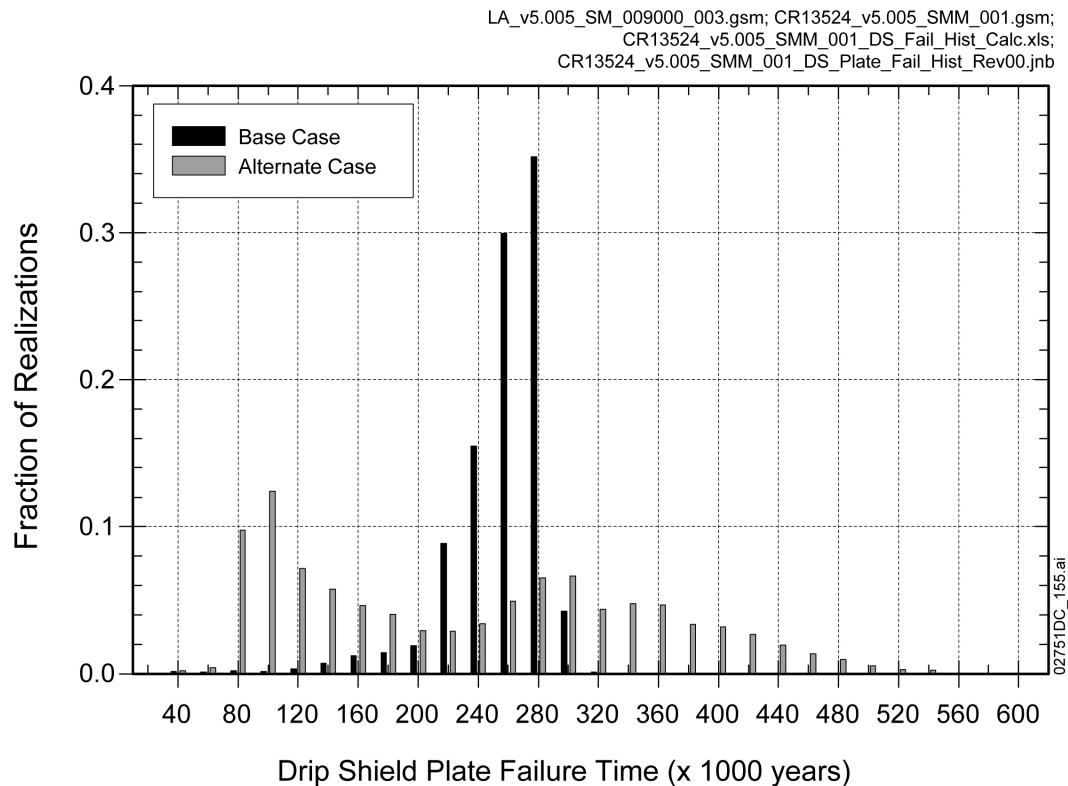## 1.4   UNCERTAINTY IN CROWN PLATE RESPONSE AND SENSITIVITY OF DOSE

The uncertainty in the plastic load capacity of the crown plate has also been maximized to indirectly encompass the uncertainty in the structural response. The boundary conditions on the crown plate are a major uncertainty in the analysis, as explained in *Seismic Consequence Abstraction* (SNL 2007b, Section 6.8.2.1). The rockfall loads on the crown plates may be nonuniform, producing an asymmetric response between the sides of the crown plate. The welds between the crown plates and the underlying framework may also constrain displacement and rotation of the crown plate to varying degrees. The resulting response of a crown plate may not match typical boundary conditions, such as fixed or simply supported, because of these effects. The range of potential boundary conditions is represented by considering two options that represent the extremes of the response: (1) a plate that is fixed to maximize the load-bearing capacity, and (2) a plate that is free to move laterally, which tends to minimize the load-bearing capacity. The resulting ultimate plastic loads as a function of plate thickness and boundary condition are presented in SAR Section 2.3.4.5.3.3.1.

The results for the plastic load capacity with fixed and laterally free boundary conditions are taken to represent the extremes of plate response at the 90th and 10th percentiles of a log-normal distribution, respectively (SNL 2007b, Figure 6-73). This approach bounds the anticipated variation in boundary conditions throughout the repository because: (1) the lower percentiles of the log-normal distribution represent the laterally free response, wherein all of the welds holding Plate-1 to the drip shield bulkheads are assumed to fail, and (2) when the plates fail in the TSPA model, they fail for every drip shield in the repository. These features maximize the impact of plate failure (and the associated access of seepage to the waste package) in comparison to the more realistic case, with a few welds failing on a limited number of drip shields. In other words, the algorithm for the seismic damage abstraction overemphasizes the extreme case with simultaneous plate failure throughout the repository.

In addition, a sensitivity analysis has demonstrated that the timing of drip shield failure from greater uncertainty in titanium corrosion rates has a negligible effect on the mean annual dose (see response to RAI 3.2.2.1.3.1-005). The sensitivity study considered both slower and faster general corrosion rates for titanium through the use of an uncertainty factor between 0.5 and 4. The multiplier has the effect of shortening or extending the lifetimes of the drip shield framework and crown plates well outside the range currently observed in model results (SAR Figure 2.4-24). Thus, if the performance assessment model were sensitive to the timing of drip shield failure, the expected annual dose for the alternate case could be higher or lower, depending on the value of the uncertainty multiplier.

Figure 9 demonstrates that applying the uncertainty multiplier to the Titanium Grade 7 corrosion rates results in both earlier and later drip shield plate failures, as evident in the bimodal appearance of the histogram in the alternate case. The figure shows that the resulting drip shield failure times varied between about 80,000 years and 500,000 years with the uncertainty factor, compared to the base case with failure times between about 140,000 years and 300,000 years. As used here, drip shield failure means failure of the crown plates as a barrier to flow.

The sensitivity calculation also demonstrated that the timing of crown plate failure has a negligible impact on repository performance. The response to RAI 3.2.2.1.3.1-005 showed that at 1 million years, the difference in the maximum of the mean annual dose between the base case and the alternate case is less than 1%. If the alternate case results were added to the results of other seismic modeling cases, the effect of the alternative case results on total mean annual dose would be negligible. Stated differently, mean annual dose is insensitive to the timing of crown plate rupture within the ranges considered for the TSPA sensitivity analysis. In addition, the sensitivity calculation assumes that all crown plates fail simultaneously, providing a more severe analysis condition than if some fraction of the crown plates fail from partial collapse.

LA_v5.005_SM_009000_003.gsm; CR13524_v5.005_SMM_001.gsm;
CR13524_v5.005_SMM_001_DS_Fail_Hist_Calc.xls;
CR13524_v5.005_SMM_001_DS_Plate_Fail_Hist_Rev00.jnb

Source: Figure 1 in the response to RAI: 3.2.2.1.3.1-005.

Figure 9.   Comparison of Drip Shield Plate Failure Time for the Base and Alternate Cases

1.5 CONCLUSIONS

The crown assembly of the drip shield is highly reinforced by the presence of five bulkheads, bulkhead longitudinal stiffeners, ten internal support plates, and ten external support plates. In effect, the crown and shoulders form a stiff box frame relative to the sidewalls. By design, the framework components in the crown of the drip shield will tend to bear more load than the plates.

The plates are welded to a robust framework that enhances their structural integrity. The enhancement is confirmed by dynamic two-dimensional simulations, which show that the crown remains intact after sidewall buckling with the maximum seismic ground motions. With an intact crown, the curved plates on the crown continue to shed seepage laterally, and the connector guide and drip shield connector assembly provide an additional barrier to any seepage that is able to flow longitudinally to the ends of the drip shield. It follows that the drip shield continues to perform as a barrier to seepage after buckling of the sidewalls.

Compared to the quasi-static model, the two-dimensional dynamic calculations provide a more accurate and direct representation of the structural response to the ground motion during a seismic event, and a more accurate simulation of drip shield failure modes. In this situation, the two-dimensional dynamic calculations have been used to verify that the quasi-static approach provides a reasonable and conservative representation of the ultimate plastic load capacity of the drip shield framework, and to confirm that snap-through of the crown was not the appropriate failure mode for performance assessment. The results from the dynamic calculations, as discussed in SAR Section 2.3.4.5.3.3.3, have confirmed these statements.

A numerical analysis was conducted for the potential for differential displacements along the drip shield to cause rupturing or tearing of the drip shield crown plate. This analysis demonstrates that a differential displacement of up to 18.2 cm per drip shield segment does not cause plate rupture. Also, the partial collapse of some segments of a drip shield while others fail is unlikely because the dynamic loads in a collapsed drift will be relatively uniform and because the crown of the drip shield is a reinforced three-dimensional structure in the axial and lateral directions (Section 1.3.2). Even if partial collapse of a few drip shield segments occurs, the ductility of the drip shield crown plate is sufficient to allow substantial differential displacement before rupture occurs. In particular, these results demonstrate that the crown plates bend but do not rupture if as many as three drip shield segments fail, and the total deflection is 54.6 cm (21.5 inches).

The uncertainty in the plastic load capacity of the plates has also been maximized to indirectly encompass the uncertainty in the structural response of the framework. The approach bounds the anticipated variation in boundary conditions throughout the repository because: (1) the lower percentiles of the log-normal distribution for plastic load capacity represent the laterally free response, wherein all of the welds holding Plate-1 to the drip shield bulkheads are assumed to fail, and (2) when the plates fail in the TSPA, they fail for every drip shield in the repository. These features maximize the impact of plate failure (and the associated access of seepage to the waste package) in comparison to the more realistic case, with a few welds failing on a limited number of drip shields. In addition, a sensitivity calculation has demonstrated that mean annual dose is insensitive to the timing of plate rupture within a range of values from 80,000 years to 500,000 years, substantially greater than the range of values from 160,000 years to 300,000 years for the base case model.

2.   COMMITMENTS TO NRC

DOE will correct a statement in SAR Section 2.3.4.5.3.3.3.

3.   DESCRIPTION OF PROPOSED LA CHANGE

The text in SAR Section 2.3.4.5.3.3.3 will be revised as follows:

> Based on these results, the limit loads determined from the quasi-static fragility analyses of the drip shield structural framework provide a reasonable and conservative estimate of ~~both the failure mode and~~ the limit loads for the complex case of strong ground motion shaking of the drip shield and rubble.

The text 'both the failure mode and' will be deleted.

4.   REFERENCES

SNL (Sandia National Laboratories) 2007a. *Mechanical Assessment of Degraded Waste Packages and Drip Shields Subject to Vibratory Ground Motion*. MDL-WIS-AC-000001 REV 00. Las Vegas, Nevada: Sandia National Laboratories. ACC: DOC.20070917.0006.

SNL 2007b. *Seismic Consequence Abstraction*. MDL-WIS-PA-000003 REV 03. Las Vegas, Nevada: Sandia National Laboratories. ACC: DOC.20070928.0011, LLR.20080414.0012..